**Geomechanics and Engineering**, *Vol. 33, No. 4 (2023) 415-425*
https://doi.org/10.12989/gae.2023.33.4.415


# Evaluation of the effect of rubble mound on pile through dynamic centrifuge model tests

Jungwon Yun[1] and Jintae Han*[2]

[1]*Department of Civil Engineering, Korea Army Academy at Yeongcheon, Yeongcheon, South Korea*
[2]*Department of Geotechnical Engineering Research, Korea Institute of Civil Engineering and Building Technology, Gyeonggi, South Korea*

(*Received November 10, 2022, Revised March 14, 2023, Accepted April 3, 2023*)

**Abstract.** Pile-supported wharves, port structures that support the upper deck, are installed on sloping ground. The sloping ground should be covered with a rubble mound or artificial blocks to protect the interior material from erosion caused by wave force. The behavior of the pile may vary during an earthquake if a rubble mound is installed on the slope. However, studies evaluating the effect of rubble mound on the pile during an earthquake are limited. Here, we performed dynamic centrifuge model tests to evaluate the dynamic behavior of piles installed in a slope reinforced with rubble mound. In the structure, some sections (single-pile, 2×2 group-pile) were selected for the experiment. The moment of the group-pile decreased by up to 26% upon installation of the rubble mound, whereas the moment of the single-pile increased by up to 41%, thus demonstrating conflicting results.

**Keywords:** centrifuge model test; pile-supported wharf; rubble mound; slope

## 1. Introduction

A wharf is a port facility at which ships are anchored. It is installed on the shore to transmit and receive cargo. Among the structural types, a pile-supported wharf is a bridge-type wharf in which piles are driven into the sloping ground and the upper deck is installed on them. This structure generally consists of piles, an upper deck supported by piles, and a sloping ground.

In general, a covering material, such as a rubble mound (RM) or artificial block, is installed on the sloping surface to protect the interior material because it may be affected by the wave force (Takahashi and Takemura 2005, McCullough *et al.* 2007, Su *et al*. 2017, Vytiniotis *et al*. 2019). However, when designing a slope reinforced with RM, only the effects of wave forces are considered in regulations, whereas the effects of earthquakes are neglected (PIANC 2001, MOF 2017). Therefore, several researchers have examined the relationship between the presence of RM and the seismic load experimentally (Memos *et al*. 2001, Cihan and Yuksel 2011, Cihan *et al*. 2012, Najma and Ghalandazadeh 2019), whereas some other researchers have conducted numerical analyses (Ye and Jeng 2013, Ye and Wang 2015). However, these studies focused on evaluating the slope stability during an earthquake in absence of pile structures.

Few studies performed experimental and numerical analyses to examine the dynamic behavior of a pile-supported wharf with RM. Takahashi and Takemura (2005) carried out a dynamic centrifuge model test to investigate the failure mechanism of a pile-supported wharf. Their experiment demonstrated that the deformation mode of the ground and structure changed as a result of varying the thickness of the sandy layer underneath the RM. In addition, Torkamani *et al*. (2014) evaluated the seismic vulnerability of pile-supported wharves through sensitivity analysis. The results indicated that the uncertainty of the internal friction angle of the RM has a great influence on differential settlements. Su *et al.* (2017) evaluated the seismic performance of pile-supported wharves using a three-dimensional finite element analysis method. Their results showed the largest slope deformation occurring at the bottom of the dike (toe), where the RM was installed. Although these studies have focused on the behavior of structures and ground, studies analyzing the effect of RMs on the interaction of the ground and pile during an earthquake are limited.

In the case of a sloping ground, the geometry of the slope causes additional acceleration amplification during an earthquake, and the response at the slope crest may be greatly amplified, up to 50 % then the free-field ground (Ashford and Sitar 2002). This may cause the slope to collapse, and a large kinematic force may be generated on the pile installed on the slope. Therefore, it is important to evaluate the effect of RMs installed on slopes on the behavior of piles during earthquakes.

In this study, dynamic centrifuge model tests were performed to evaluate the effects of an RM installed on a slope on the behavior of the piles during an earthquake. First, the dependence of the frequency characteristics and natural period of the pile structure on the RM, were analyzed. Then, the acceleration response of the ground and pile, the lateral soil resistance (p), and the pile moment were

*Corresponding author, Ph.D.
E-mail: jimmyhan@kict.re.kr



ISSN: 2005-307X (Print), 2092-6219 (Online)

analyzed to obtain insights into the dynamic interaction between the ground and pile.

## 2. Materials and method

A centrifuge model test can replicate the actual stress conditions on the ground by increasing the gravitational acceleration n times in a 1/n scaled model (n: scale factor). This type of test is widely used in geotechnical engineering largely because unlike real scale experiments, it is an inexpensive approach for evaluating the behavior of geotechnical structures (Haigh and Madabhushi 2011, Lees and Richards 2011, Yoo *et al*. 2013, Kim and Choi 2017, Yoo *et al*. 2017, Kwon and Yoo 2019, Yun *et al.* 2019, Kwon and Yoo 2020, Yun *et al*. 2022b).

A geo-centrifuge experimenter from the Korea Advanced Institute of Sciences and Technology (KAIST) was used in this study. The rotation radius of the machine is 5 m, and the test can be performed at a maximum of 240 g-ton (Kim *et al*. 2013). The model soil box used in the experiment is a square equivalent shear beam box with a length, width, and height of 49, 49, and 63 cm, respectively (Kim *et al*. 2013, Lee *et al*. 2013).

The experimental model was selected by modifying some sections of a pile-supported wharf located in Pohang, Korea. As shown in Fig. 1, two models were assumed for the ground: 1) a model with a single sand layer without RM and 2) a model with RM. The depth of RM was constructed to be about 2m thick based on the prototype by referring to the McCullough (2007) experimental model (JCB01, SMS02). Each model consist of a single and a group-pile (2×2) and was produced at a 1/34 scale. In general, it is preferable to reduce the diameter and thickness of the pile by a scale factor (n) when manufacturing a reduced model. However, the thickness of the pile can become extremely small, making it difficult to manufacture it. Therefore, model specifications were calculated considering flexural stiffness (EI) as in Eq. (1) to simulate the lateral behavior of piles (Ko *et al*. 2019). Table 1 shows the properties of the derived model and prototype structure.

$$n^4 = \frac{EI_{prototype}}{EI_{model}} \quad (1)$$

where n is the scale factor (in this study: 34), E is the elastic modulus of the pile, and I is the second moment of area. In this experiment, dry silica sand was air-pluviated to form a relative density of approximately 50%. In this experiment, a medium ground with a relative density of 50% was created.

This is because, when the relative density is too low, settlement occurs significantly during shaking making it difficult to maintain the slope, and when relative density is too high, it becomes difficult to clearly examine the applicability of the RM. Table 2 presents the properties of silica sand. Ovesen (1979) reported that the particle size had no effect on the pile diameter in a centrifuge model test if the pile diameter was at least 35 times larger than the average particle diameter. In this experiment, the pile diameter was approximately 83 times the median ($D_{50}$) particle diameter of silica sand, satisfying Ovesen's criteria.

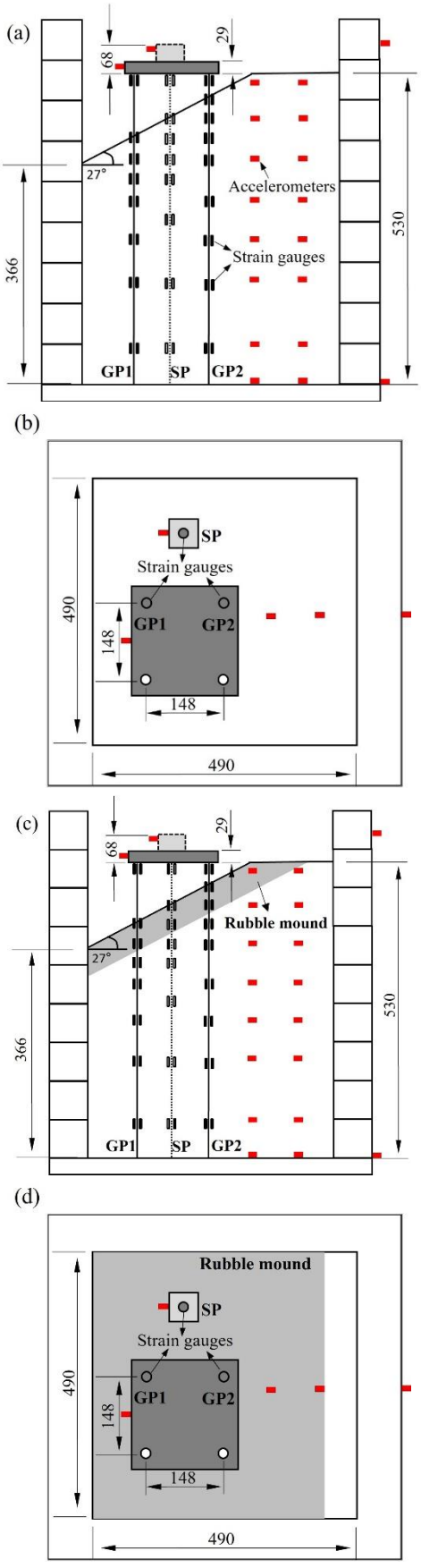


Fig. 1 Model cross-section and plan views; (a), (b) model without rubble mound; (c), (d) model with rubble mound (in model scale, unit: mm)

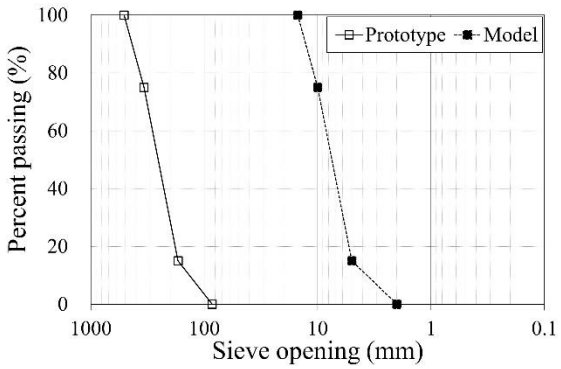


Fig. 2 Rock gradations used in the models

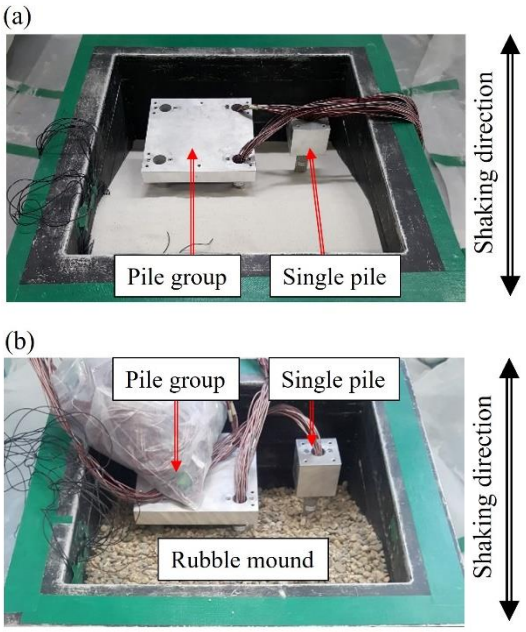


Fig. 3 Experimental model: (a) Model without rubble mound and (b) Model with rubble mound

In the case of an RM installed on the slope, the particle diameter that is mainly used in practice (10–50 cm) was selected. As shown in Fig. 2, it was produced as a 1/34 scale model. Table 3 presents the properties of rubble mound.

Accelerometers and strain gauges were installed to measure the ground and structure acceleration and the pile strain, respectively (Figure 1). Figure 3(a) shows a model constructed as a single layer without RM, whereas Figure 3(b) shows a model with RM installed. For seismic motions, sinusoidal signals with a frequency of 1.5 Hz (period: 0.67 s) and Gyeongju earthquake with various frequency ranges were used. In a sinusoidal signal, seismic motions with a constant increasing and decreasing amplitude are produced. A sinusoidal signal with a small amplitude region (0.06 g) was excited for the phase analysis of the model. The Gyeongju earthquake, at a magnitude of 5.8, is the largest earthquake ever recorded in Gyeongju, South Korea. The earthquake occurred in 2016, and it was produced by a spectrum matching the original Gyeongju earthquake according to the criteria presented by MOIS

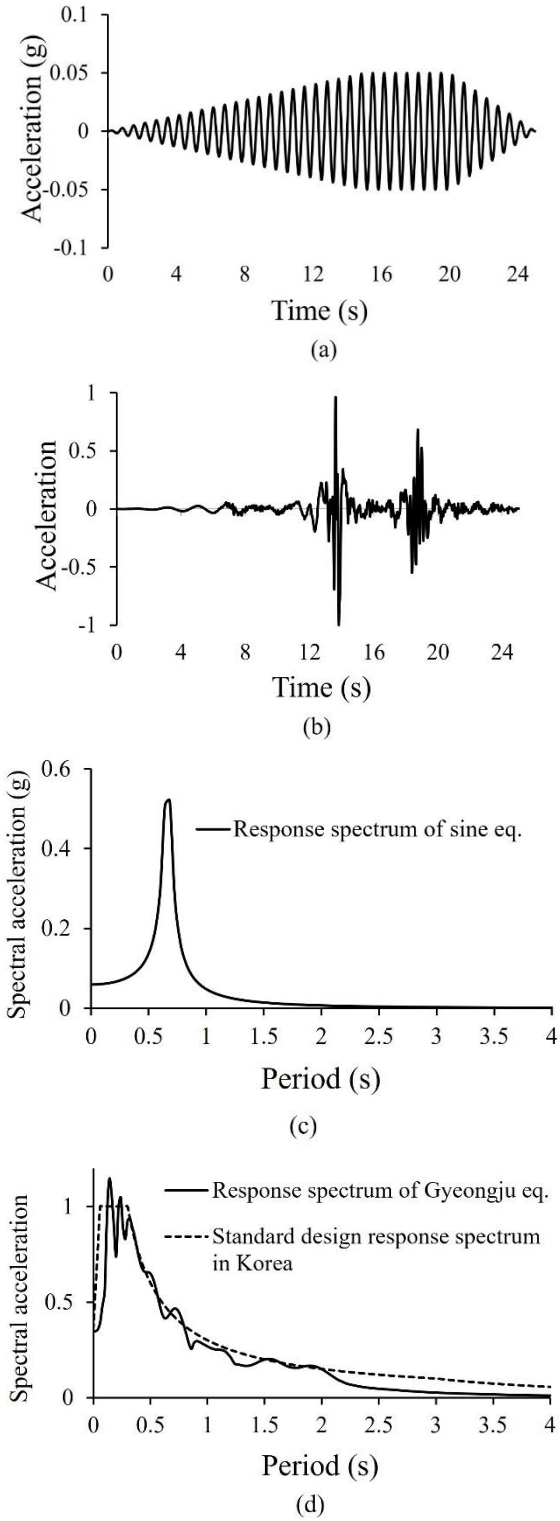


Fig. 4 Time history curve of input earthquake and acceleration response spectrum: (a) time history of sinusoidal signal, (b) Normalized time history of Gyeongju earthquake, (c) response spectrum of sinusoidal signal and (d) Normalized response spectrum of Gyeongju earthquake

(2017). As shown in Table 4, seismic motion with an amplitude of 0.07–0.22 g was excited to analyze the model's behavior in the case of the Gyeongju earthquake.

Table 1 Prototype and model properties (scale factor = 34)

| | | Prototype (steel) | Model (aluminum) |
|---|---|---|---|
| Pile | Diameter (mm) | 914 | 25 |
| | Thickness (mm) | 14 | 2 |
| | Length (mm) | 18,000 | 530 |
| | Density (kN·m$^{-3}$) | 78.5 | 26.4 |
| | Flexural rigidity (kN·m$^2$) | $8.94 \times 10^5$ | 0.669 |
| Deck of GP | Thickness (mm) | 1,000 | 29 |
| | Density (kN·m$^{-3}$) | 24.5 | 26.4 |
| Deck of SP | Thickness (mm) | 2,300 | 68 |
| | Density (kN·m$^{-3}$) | 24.5 | 26.4 |

Table 2 Basic properties of the silica sand used in the experiments

| Soil property | USCS | $C_c$ | $C_u$ | $G_s$ | $\gamma_{d.max}$ (kN·m$^{-3}$) | $\gamma_{d.min}$ (kN·m$^{-3}$) |
|---|---|---|---|---|---|---|
| Silica sand | SP | 1.16 | 1.96 | 2.63 | 16.5 | 12.4 |

Table 3 Basic properties of the rubble mound used in the experiments

| Soil property | USCS | $C_c$ | $C_u$ | $G_s$ | $\gamma_{d.max}$ (kN·m$^{-3}$) | $\gamma_{d.min}$ (kN·m$^{-3}$) |
|---|---|---|---|---|---|---|
| Rubble mound | GP | 1.09 | 2.2 | 2.65 | 17.7 | 16.2 |

Table 4 Base input seismic motion for each model

| Model | | Model without rubble mound | Model with rubble mound |
|---|---|---|---|
| Relative density (%) | | 50 | 50 |
| Input base acceleration amplitude (g) | Sinusoidal signal | 0.06 | 0.06 |
| | Gyeongju earthquake | 0.07 | 0.07 |
| | | 0.10 | 0.10 |
| | | 0.14 | 0.15 |
| | | 0.18 | 0.18 |
| | | 0.22 | 0.21 |

Figs. 4(a) and 4(c) show the acceleration time history curve and the acceleration response spectrum curve of the sinusoidal signal. Figs. 4(b) and 4(d) show the normalized acceleration time history curve and acceleration response spectrum curve of the Gyeongju earthquake.

## 3. Results and discussion

### *3.1 Seismic response of the centrifuge model tests*

Fig. 5 shows the seismic response of the models with and without RM to the Gyeongju earthquake. The graph in Fig. 5(a) compares the ratio of response spectrum (RRS) of

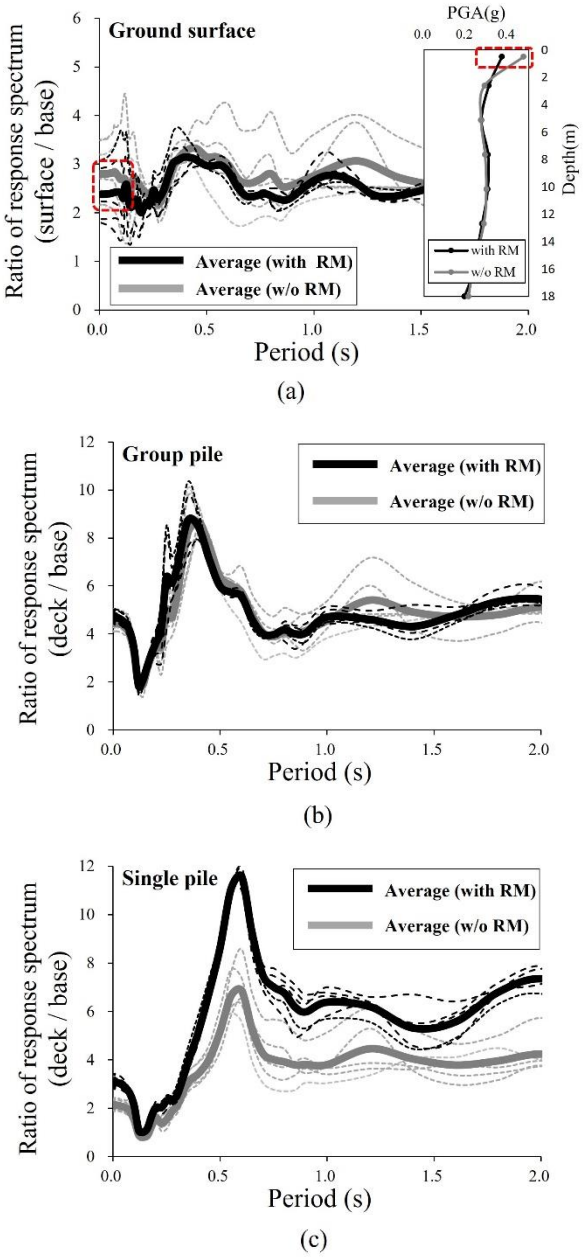


Fig. 5 Ratio of response spectrum (RRS) with and without rubble mound (Gyeongju earthquake): (a) RRS between base and ground surface, (b) RRS between base and deck (group-pile) and (c) RRS between base and deck (single-pile)

the base and the ground surface according to the magnitude of the input acceleration. The black lines are the ground response, and the bold black line is the average ground response when RM is installed, whereas the gray lines are the ground response and the bold gray line is the average ground response when the RM is not installed. Also, Fig. 5(a) on the right shows the peak ground acceleration (PGA) according to the depth. Most of the RRS in Fig. 5(a) are higher than 2, and the acceleration response at the ground surface is more than double than at the base. This indicates the occurrence of ground amplification during the earthquake. In particular, a significant acceleration response

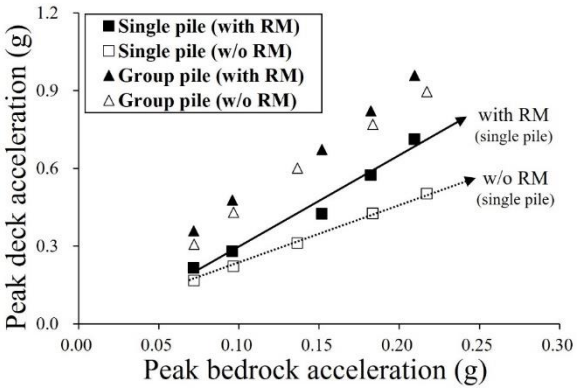


Fig. 6 Peak deck acceleration with and without rubble mound

occurred in the ground where the RM was not installed, and a difference of more than 20% occurred at the ground surface. Generally, the ground amplification occurs more significantly when the upper ground is loose due to difference in stiffness of the ground.

Fig. 5(b) shows the RRS of the base and the upper deck in group-pile model, and Fig. 5(c) shows the RRS of the base and the upper deck in single-pile model. The graph shows the average response according to the magnitude of the input acceleration. The bold black line is the average response when the RM is installed, and the bold gray line is the response when the RM is not installed. There was no significant difference in the RRS of the group-piles with and without the RM, with the largest amplification ranging 0.35–0.4 s (Fig. 5(b)). However, a significant difference was observed in the RRS of the single pile with and without the RM (Fig. 5(c)). In particular, the RRS was at a maximum of 7 when the RM was not installed, and maximum a 12 when the RM was installed. However, in the case of single piles with and without the RM, the greatest amplification was observed at approximately 0.6 s. This implies that the installation of the RM does not affect the change of natural period of the structure. In addition, it was found that the natural period of the group-pile model was smaller than that of the single pile model. This is because the four piles in the group-pile model act as a unit and the pile cap is fixed, resulting in an increase in the overall stiffness of the system.

Fig. 6 compares the deck acceleration response according to the magnitude of the input base acceleration based on the results of Fig. 5. The figure shows the maximum acceleration for each response and compares the response of each structure with and without the RM. There was no significant difference in the acceleration response of the group-pile with and without the RM, whereas there was a significant difference in the acceleration response of the single pile with and without the RM. In particular, the acceleration response increased by approximately 40% when the RM was installed in the single-pile model.

In summary, the natural period of the structure did not change when installing the RM, but there was a difference of approximately 40% in the acceleration response when installing the RM only in the single-pile structure. In order to explain the above phenomenon, a comprehensive analysis of the interaction of the soil and pile, which is explained in the next section, is required.

### *3.2 Dynamic interaction of soil and the pile*

Figs. 7 and 8 compare the acceleration time history of the upper deck and the ground surface to analyze the interaction between the soil and structure. Fig. 7 represents the results of a sinusoidal signal to clearly examine the acceleration phase of the soil and structure (input base acceleration: 0.06 g, 15–20 s). In addition, the acceleration gradient between the deck and ground surface is shown in the upper right corner of each figure. The acceleration gradient is represented by the x-axis showing the ground acceleration time history and the y-axis showing the deck acceleration time history. The average gradient is indicated within each graph. Figs. 7(a) and 7(b) show the responses of the single- and group-pile structures, respectively, without RM. Figs. 7(c) and 7(d) show the responses of the single- and group-pile structures, respectively, with RM.

As shown in Fig. 7(a), the ground surface and upper deck had opposite phases in a single-pile model without an RM. This finding implies that the phase direction of the kinematic force caused by the ground movement and the inertial force caused by the mass of the deck did not match. Therefore, the acceleration gradient was derived in the negative (-) direction. In the case of the single-pile structure, the soil and the pile have opposite phases because the pile pushes the ground by the inertial force of the upper deck and the pile is supported by the surrounding ground. Tokimatsu *et al.* (2005) performed a 1-g shaking table test on a pile structure and measured the inertial force at the upper deck and the earth's pressure during an earthquake.

They reported that the phases of the inertial force and the ground kinematic force in the dry ground model do not match. However, as shown in Fig. 7(b), the phase of the ground surface and upper deck were consistent in the group-pile model without RM, i.e., the direction of the kinematic force caused by the ground movement and the inertial force caused by the mass of the deck were the same. Thus, the acceleration gradient was derived in the positive (+) direction. In the group-pile model, the pile head is fixed, and the number of piles increases. Since the pile has high stiffness, the phase difference between the ground and the deck decreases as the ground and the pile behave integrally (Tran *et al*. 2022). However, no significant difference was observed in the behavior of the piles in the models with RM (Figs. 7(c) and 7(d)) and without RM (Figs. 7(a) and 7(b)). This is because the frequency of the given sinusoidal signal is fixed at 1.5 Hz, making it impossible to properly reflect the response characteristics of the soil that vary with input frequency.

Fig. 8 shows the acceleration time history of the Gyeongju earthquake (input base acceleration: 0.18 g, 1-5s). As shown in Figs. 8(a) and 8(c), the ground surface and upper deck had opposite phases in a single-pile model, and the acceleration gradient was derived in the negative (-) direction. However, as shown in Figs. 8(b) and 8(d), the phase of the ground surface and upper deck were consistent

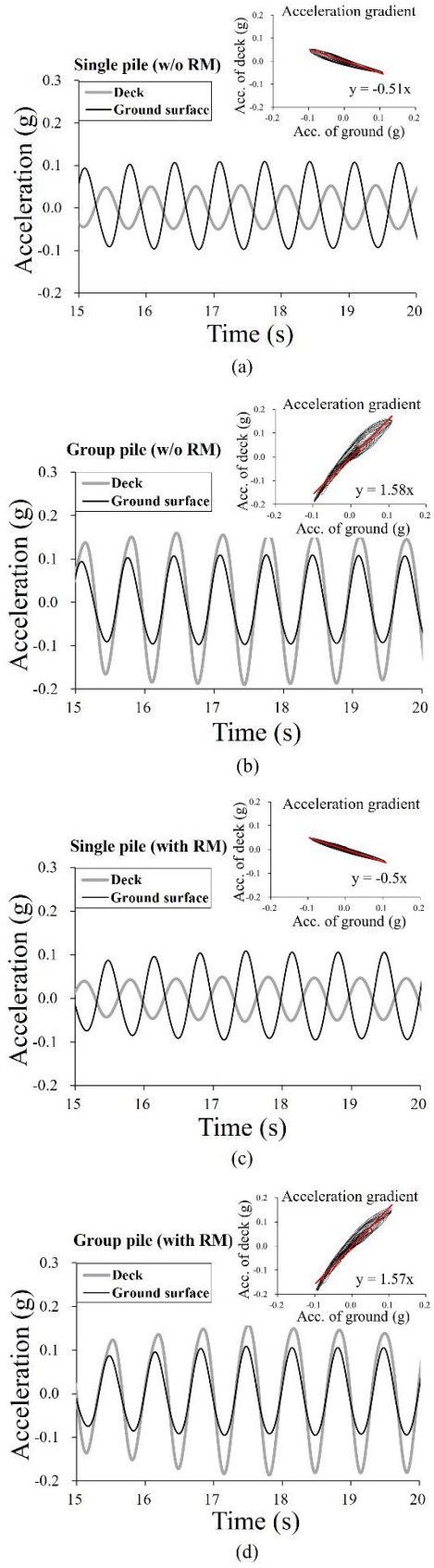


Fig. 7 Acceleration relationship between deck and ground surface (Sinusoidal signal, 0.06 g): (a) Single-pile without rubble mound, (b) Group-pile without rubble mound, (c) Single-pile with rubble mound and (d) Group-pile with rubble mound

in group-pile model, and the acceleration gradient was derived in the positive (+) direction. Although the results are somewhat unclear compared to the sinusoidal result, it was found that the similar trend was observed even when subjected to the Gyeongju earthquake. Furthermore, comparing the model without RM (Figs. 8(a) and 8(b)) and model with RM (Figs. 8(c) and 8(d)), the absolute value of the acceleration gradient was found to be larger in the model with RM. As previously explained in Fig. 5(a), when RM is installed, the ground acceleration response decreases, which appears to increase the acceleration gradient.

Fig. 9 shows the lateral soil resistance (p) according to the depth and acceleration amplitude (base input acceleration: 0.18 g; Gyeongju earthquake). Figs. 9(a) and 9(b) show the results for the group-pile and single-pile models, respectively. The soil resistances were derived at the time of maximum deformation in the pile. The lateral soil resistance was derived using Eq. (2).

$$p = \frac{d^2}{dz^2} M(z) \tag{2}$$

where M(z) indicates the pile moment for each depth measured through the experiment. The figures show the peak ground acceleration response in the downward direction. The peak ground acceleration was obtained as 0.41 g for the case without RM model and 0.34 g for the case with RM model. Additionally, the figure shows the peak acceleration response at the deck. Based on the results obtained in Figs. 7 and 8, the peak acceleration response was shown for the case where the direction of the ground surface and deck acceleration are consistent in the case of group-pile model, and for the case where the direction of the ground surface and deck acceleration responses are opposite in the case of single-pile model.

As shown in the GP1 in Fig. 9(a), the lateral soil resistance increased to about 3D depth from the ground surface when the RM was installed on the ground surface. Here, D refers to the pile diameter. In particular, it increased by about 27% near the ground surface. This is because RM is installed on the upper part of the ground, the ground stiffness increases, leading to an increase in lateral soil resistance at this location. However, the lateral soil resistance decreased when the depth was more than the 3D depth when the RM was installed on the ground surface. In particular, it decreased by about 32% at the 4D depth from the ground surface. Although the phases of the kinematic force induced by soil movement and the inertial force of the deck mass are similar in the group-pile model, the magnitudes of acceleration are different. Therefore, the RM at the slope surface constrains the movement of the pile, and the inertial force of the upper deck is not transmitted to the lower part of the pile. As a result, as the deformation of the pile decreases, the lateral soil resistance also decreases.

As shown in Fig. 9(b), the lateral soil resistance in the single-pile model increased to about 4D depth when the RM was installed on the slope surface. In particular, it increased by about 84% near the ground surface. This is because RM is installed in the ground surface, as shown in Fig. 9(a), which increases the stiffness and lateral soil resistance of the soil. In addition, in the case of single-pile, the phase of

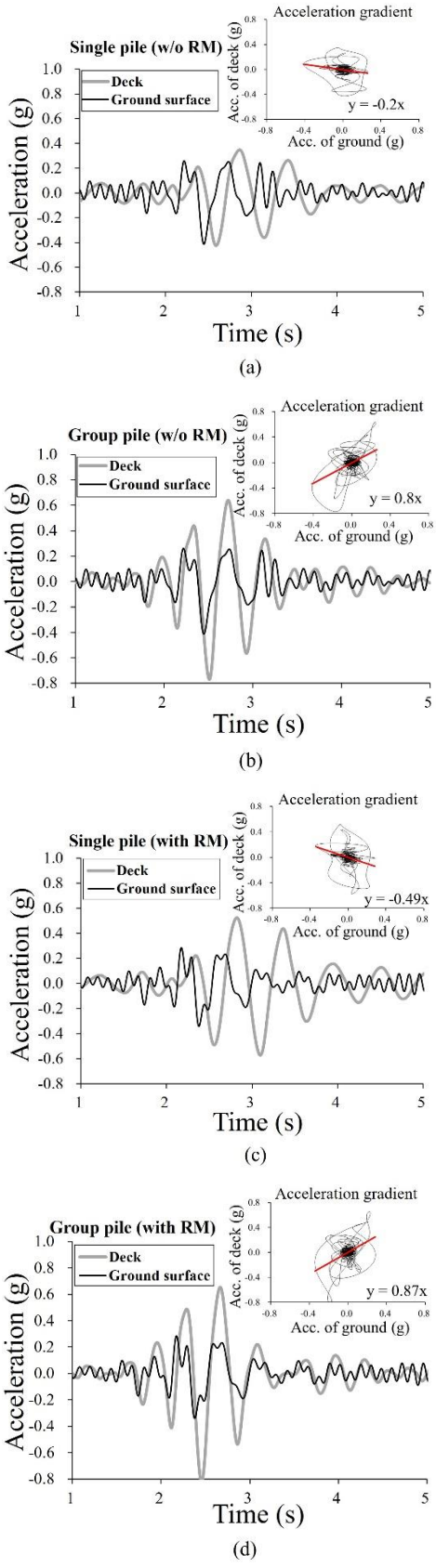


Fig. 8 Acceleration relationship between deck and ground surface (Gyeongju earthquake, 0.18 g): (a) Single-pile without rubble mound, (b) Group-pile without rubble mound, (c) Single-pile with rubble mound and (d) Group-pile with rubble mound

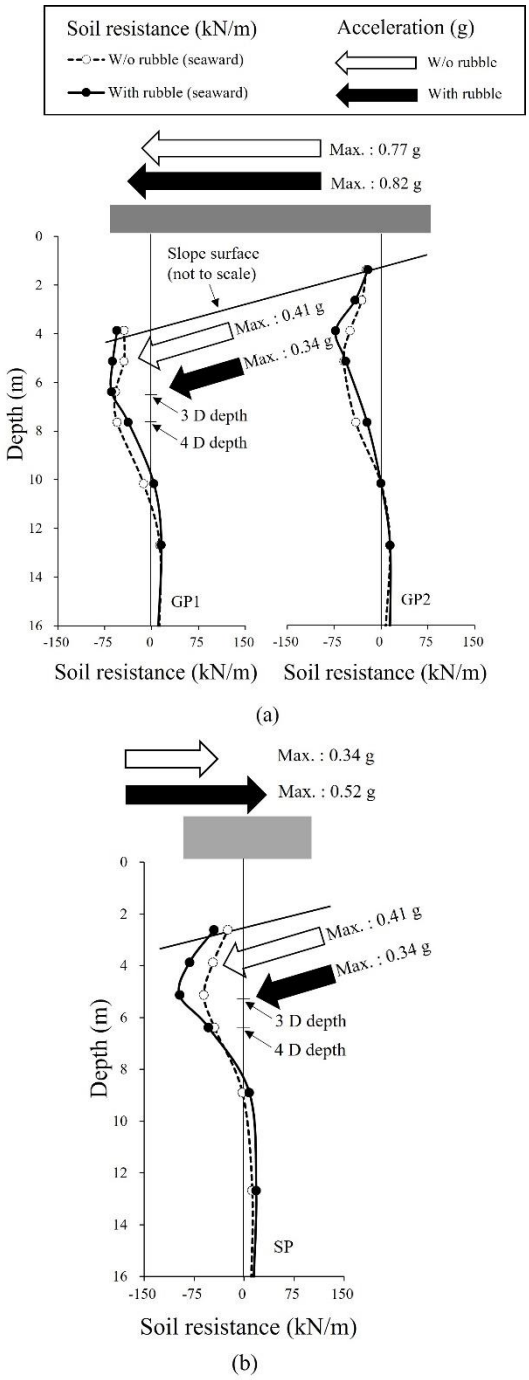


Fig. 9 Lateral soil resistance distribution curves and acceleration amplitude with and without rubble mound (Gyeongju earthquake, 0.18 g): (a) Group-pile and (b) Single-pile

the kinematic force caused by ground acceleration and the inertial force caused by deck mass are opposite, so the kinematic force acts as a resisting force on the pile. Therefore, when RM is installed, the ground acceleration and kinematic force decreases, and the deck inertial force in the opposite direction of the ground kinematic force increases. As a results, it is determined that the deformation of the pile increased and the lateral soil resistance also increases.

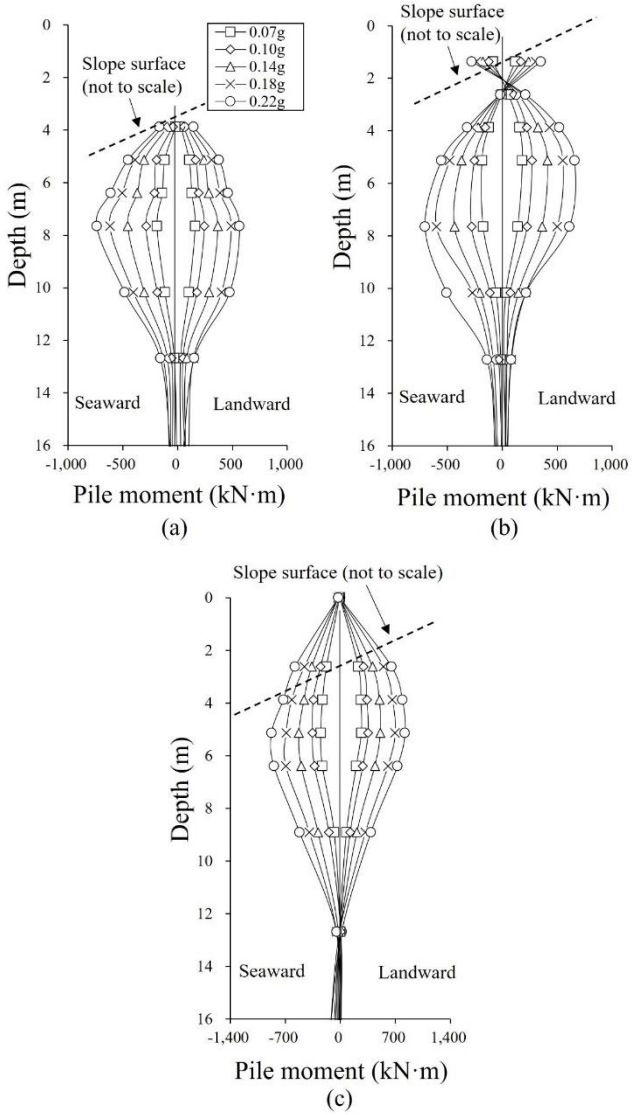


Fig. 10 Depth profile of the pile bending moment without rubble mound: (a) Group-pile (GP1), (b) Group-pile (GP2) and (c) Single-pile (SP)

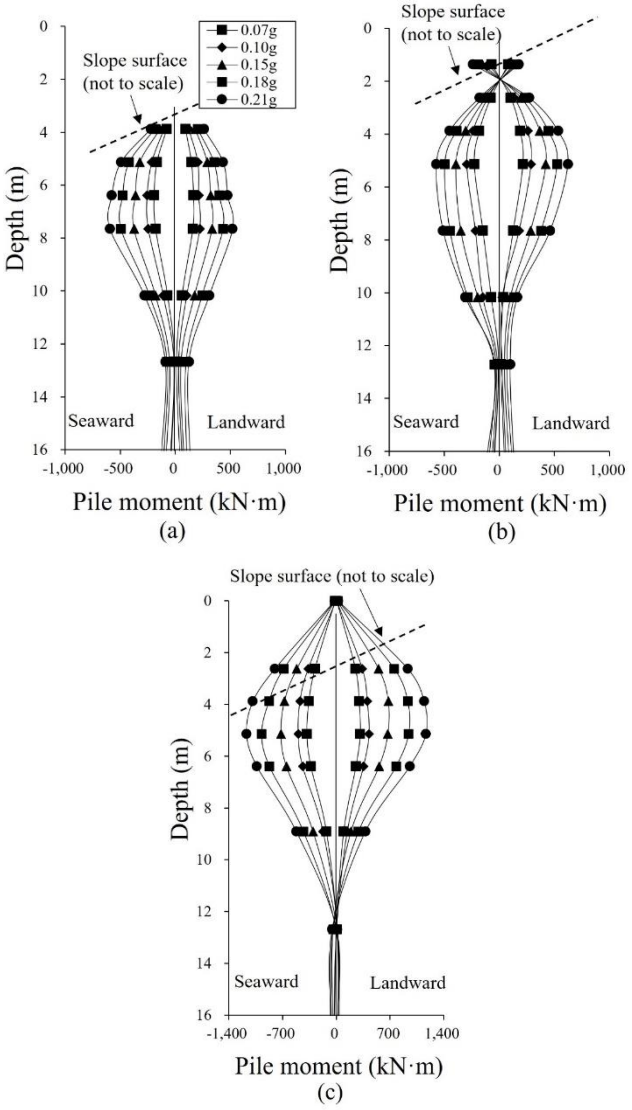


Fig. 11 Depth profile of the pile bending moment with rubble mound: (a) Group-pile (GP1), (b) Group-pile (GP2) and (c) Single-pile (SP)

Figs. 10 and 11 show the depth profile of the pile bending moment according to the input base acceleration amplitude (Gyeongju earthquake). Figs. 10(a) and 10(b) show the response of the group-pile without the RM. Figure 10(c) shows the response of the single-pile without the RM. As shown in Fig. 10, the pile moment increases with the increase in input acceleration. In the single-pile model, the moment at the top (0 m) was derived as 0 because the top of the pile was a free rotation condition. However, in the group-pile model, the moment at the top of the pile was more than 0 because the top was a fixed head condition (GP2). An error occurred in the measuring instrument at the top of GP1. In addition, the moment varies according to the direction of pile movement. In particular, the maximum moment generation position in the case of GP2 was higher when the pile moved landward than when it moved seaward. This is because when the pile moves in the landward direction, the soil confining pressure due to the slope is greater than when it moves in the seaward direction. Figs. 11(a) and 11(b) show the response of the group-pile with RM, and Fig. 11(c) shows the response of the single-pile with RM. As shown in the figure, the pile moment increases with the increase in the input acceleration in the single-pile model as well. The maximum moment at the GP2 was derived at a similar position in both the cases of the pile moving in the landward and seaward directions. The difference in the moment according to the direction of pile behavior decreased after installing the RM. This is because the inertial force of the upper deck is not transmitted to the lower part when the RM is installed as described above.

Fig. 12 shows the depth profile of the pile bending moment with and without the RM (base input acceleration: 0.18 g, Gyeongju earthquake). Figs. 12(a) and 12(b) show the response of the group-pile model, whereas Fig. 12(c) shows the response of the single-pile model. Each figure

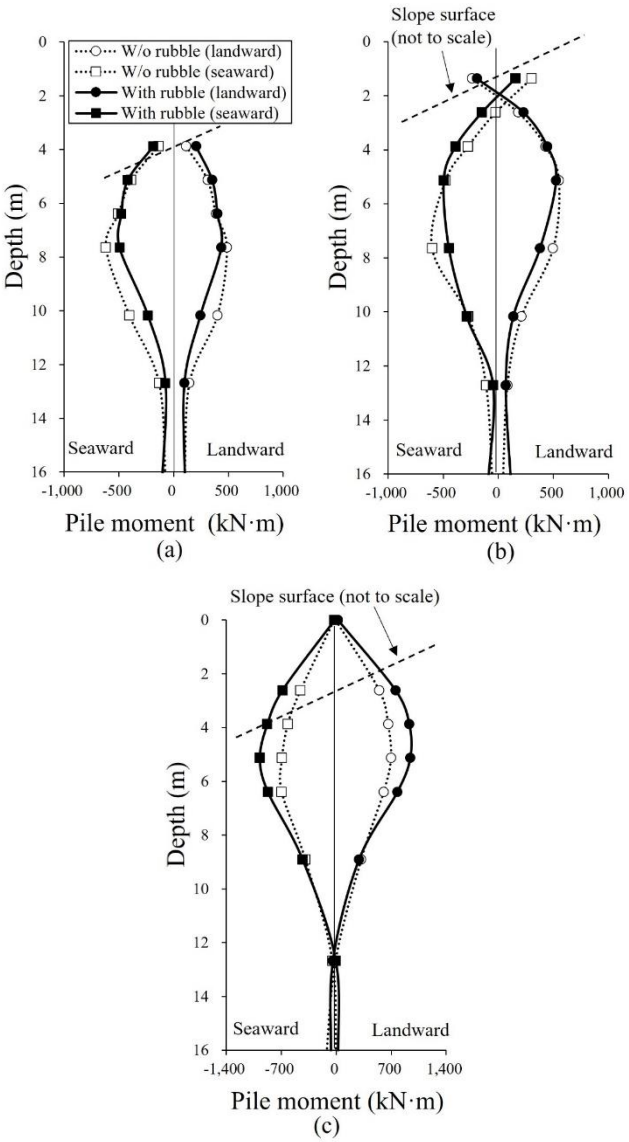


Fig. 12 Depth profile of the pile bending moment with and without rubble mound: (a) Group-pile (GP1), (b) Group-pile (GP2) and (c) Single-pile (SP)

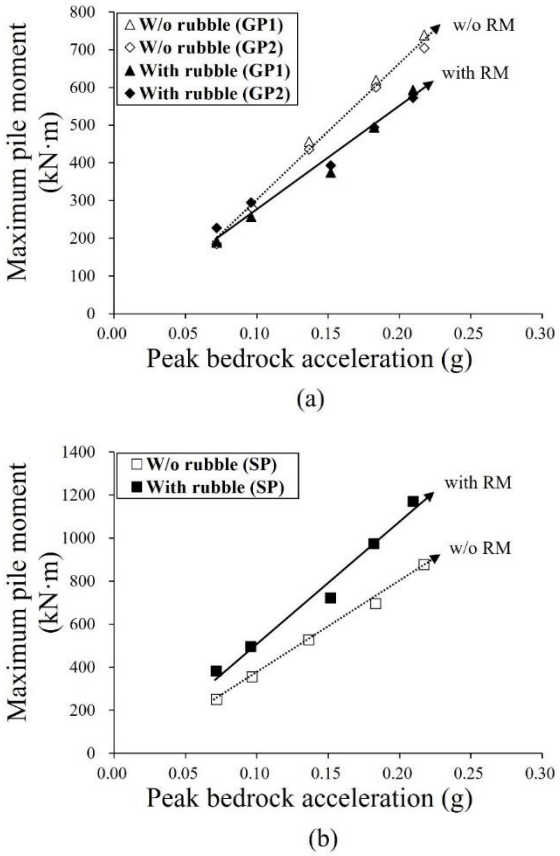


Fig. 13 Maximum pile moment with and without rubble mound: (a) Group-pile and (b) Single-pile

shows the moment according to the depth at the time when the maximum moment occurs. The results of the group-pile (GP1 and GP2) model show that the moment was reduced by up to 26% at the lower part of the ground (8 m) when the RM was installed. This is because although the phases of the kinematic force induced by soil movement and the inertial force of the deck mass are similar in the group-pile model, the magnitudes of acceleration are different. Therefore, the RM constrains the pile movement, reducing the pile moment of the lower part of the ground. However, the results of the single-pile model show that the moment increased at all depths when the RM was installed. In particular, the pile moment increased by up to 41% when the RM was installed at a depth of 5 m. In the case of the single-pile model, the phase of the ground kinematic force and the inertial force of the deck are opposite, so the ground kinematic force acts as a resisting force on the pile. As a result, when installing the RM, the ground acceleration and kinematic force decrease, leading to an increase in the inertial force of deck and moment of pile (Fig. 9(b)).

Fig. 13 shows the maximum pile moment according to the input acceleration amplitude (Gyeongju earthquake). Figs. 13(a) and 13(b) show the response of group-pile and single-pile with and without the RM when the pile moves in the seaward direction, respectively. As shown in the figure, the moment response in the group-pile model decreased when an RM was installed, whereas the moment response in the single-pile model significantly increased when RM was installed. Even when the input acceleration is different, the same trend was derived as described above. Therefore, they show conflicting results according to the dynamic interaction between the ground and piles when the pile was installed on the slope reinforced with or without an RM.

In this study, conflicting results were obtained when RM was installed in the pile-supported wharf. This is because the phase characteristics between kinematic force caused by soil movement and inertial force of the upper mass in the single and group-piles, as shown in Fig. 9. However, only the inertial force of the deck mass is considered in the seismic design of the pile-supported wharf. For example, equivalent static and response spectrum analysis are currently used in practice, and the effect of kinematic force is not considered (Yun and Han 2021, Yun *et al*. 2022a). If the kinematic force is not considered, the response of the structure can be over/underestimated when installing the RM. This study delved into the effect of kinematic force on

single and group-piles with and without the RM; insights that were gleaned will be useful in taking into account the kinematic force to improve seismic design efforts.

In general, since the pile-supported wharf is port structure, the behavior of the pile may be changed by wave, current, tidal and even differential water pressure. However, since the studies analyzing the effect of RM on piles during earthquake are insufficient, this study was conducted only in consideration of earthquake without considering other factors.

## 4. Conclusions

In this study, dynamic centrifuge model tests were performed to evaluate the effect of an RM installed on a slope on the behavior of the pile during an earthquake. The interaction between the ground and the structure with and without the RM was analyzed by comprehensively examining the response of the ground and the structure. The following conclusions were drawn.

In the single-pile model, the kinematic force induced by soil movement and the inertial force of the deck mass were in phase opposition. However, the phase difference was lower in the group-pile model, which can be attributed to the fact that the pile head fixed and the stiffness of the pile increased.

In the group-pile model, the lateral soil resistance decreased by ~32% in the lower part of the ground when the RM was installed, compared to that in the case in which the RM was not installed. In this model, the kinematic force induced by soil movement and the inertial force of the deck mass were in phase, and the RM at the slope surface constrained the movement of the pile. Therefore, the inertial force of the upper deck was not transmitted to the lower part of the pile. As a result, the deformation of the pile decreases and lateral soil resistance also decreases.

In the single-pile model, the lateral soil resistance increased by ~84% when the RM was installed, compared to that in the case in which the RM was not installed. In this model, the kinematic force induced by soil movement and the inertial force of the deck mass were in opposition phase, so the kinematic force acts as a resting force on the pile. Therefore, when RM is installed, the ground kinematic force decreases, resulting in an increase in the inertial force of the deck. As a result, the deformation of the pile increases and lateral soil resistance also increases.

In the group-pile model, the pile moment decreased by up to 26% when the RM was installed. This is because that the RM constrains the pile movement, reducing the pile moment of the lower part of the ground. Conversely, in the single-pile model, the pile moment increased by up to 41% when the RM was installed. When the rubble mound is installed on a slope, the ground acceleration and kinematic force decrease, and, the inertial forces of the deck and pile moment increase.

In practice, only the inertial force of the upper deck is considered in the design of a pile-supported wharf with an RM, whereas the kinematic force of the ground is neglected. However, the inertial force of the upper deck and the kinematic force of the ground act together during an earthquake, and the phase direction of two forces may be different between the single-pile and group-pile models. This leads to conflicting results when the RM is installed on the single and group-piles.

## Acknowledgments

This research was funded by the “Korea Institute of Civil Engineering and Building Technology, grant number 20230132-001” and “Korea Institute of Marine Science & Technology Promotion (KIMST), grant number 2016-0065”.

## References

Ashford, S.A. and Sitar, N. (2002), “Simplified method for evaluating seismic stability of steep slopes”, *J. Geotech. Geoenviron. Eng.,* **128**(2), 119-128. https://doi.org/10.1061/(ASCE)1090-0241(2002)128:2(119).

Cihan, K. and Yuksel, Y. (2011), “Deformation of rubble-mound breakwaters under cyclic loads”, *Coast. Eng*., **58**(6), 528-539. https://doi.org/10.1016/j.coastaleng.2011.02.002.

Cihan, K., Yuksel, Y., Berilgen, M. and Cevik, E.O. (2012), “Behavior of homogenous rubble mound breakwaters materials under cyclic loads”, *Soil Dyn. Earthq. Eng*., **34**(1), 1-10. https://doi.org/10.1016/j.soildyn.2011.10.009.

Haigh, S.K. and Gopal Madabhushi, S.P. (2011), “Centrifuge modelling of pile-soil interaction in liquefiable slopes”, *Geomech. Eng.,* **3**(1), 1-16. https://doi.org/10.12989/gae.2011.3.1.001.

Heidary-Torkamani, H., Bargi, K., Amirabadi, R. and McCllough, N. J. (2014), “Fragility estimation and sensitivity analysis of an idealized pile-supported wharf with batter piles”, *Soil Dyn. Earthq. Eng*., **61**, 92-106. http://doi.org/10.1016/j.soildyn.2014.01.024.

Kim, D.S., Kim, N.R., Choo, Y.W. and Cho, G.C. (2013), “A newly developed state-of-the-art geotechnical centrifuge in Korea”, *KSCE J. Civil Eng.,* **17**(1), 77-84. http://doi.org/10.1007/s12205-013-1350-5.

Kim, Y.S. and Choi, J.I. (2017), “Nonlinear numerical analyses of a pile-soil system under sinusoidal bedrock loadings verifying centrifuge model test results”, *Geomech. Eng*., **12**(2), 239-255. https://doi.org/10.12989/gae.2017.12.2.239.

Ko, K.W., Park, H.J., Ha, J.G., Jin, S., Song, Y.H., Song, M.J. and Kim, D.S. (2019), “Evaluation of dynamic bending moment of disconnected piled raft via centrifuge tests”, *Can. Geotech. J*., **56**(12), 1917-1928. http://doi.org/10.1139/cgj-2018-0248.

Kwon, S.Y. and Yoo, M. (2019), “Evaluation of dynamic soil-pile-structure interactive behavior in dry sand by 3D numerical simulation”, *Appl. Sci.,* **9**(13), 2612. https://doi.org/10.3390/app9132612.

Kwon, S.Y. and Yoo, M. (2020). “Study on the dynamic soil-pile-structure interactive behavior in liquefiable sand by 3D numerical simulation”, *Appl. Sci.*, **10**(8), 2723. https://doi.org/10.3390/app10082723.

Lee, S.H., Choo, Y.W. and Kim, D.S. (2013), “Performance of an equivalent shear beam (ESB) model container for dynamic geotechnical centrifuge tests”, *Soil Dyn. Earthq. Eng*., **44**, 102-114. http://doi.org/10.1016/j.soildyn.2012.09.008.

Lees, A.S. and Richards, D.J. (2011), “Centrifuge modelling of temporary roadway systems subject to rolling type loading”, *Geomech. Eng.,* **3**(1), 45-59.

https://doi.org/10.12989/gae.2011.3.1.045.
McCullough, N.J., Dickenson, S.E., Schlechter, S.M. and Boland, J.C. (2007), "Centrifuge seismic modeling of pile-supported wharves", *Geotech. Test. J.,* **30**(5), 349-359. https://doi.org/10.1520/GTJ14066.
Memos, C., Bouckovalas, G. and Tsiachris, A. (2001), "Stability of rubble-mound breakwaters under seismic action", *In Coast. Eng., 2000*, 1585-1598.
MOF (Ministry of Oceans and Fisheries) (2017), Design standards of harbour and port. Sejong, Korea: Ministry of Oceans and Fisheries (in Korean).
MOIS (Ministry of the Interior and Safety) (2017), Announcement of common application of seismic design criteria. Sejong, Korea: Ministry of the Interior and Safety (in Korean).
Najma, A. and Ghalandarzadeh, A. (2019), "Experimental study on the seismic behavior of composite breakwaters located on liquefiable seabed", *Ocean Eng*., **186**, 106127. https://doi.org/10.1016/j.oceaneng.2019.106127.
Ovesen, N.K. (1979), "The scaling law relationship-panel discussion", *Proceedings of the 7th European Conference on Soil Mechanics and Foundation Engineering*.
PIANC (Permanent International Association for Navigation Congresses) (2001), Seismic design guidelines for port structures. Rotterdam, Netherlands: International Navigation Association.
Su, L., Lu, J., Elgamal, A. and Arulmoli, A.K. (2017), "Seismic performance of a pile-supported wharf: Three-dimensional finite element simulation.", *Soil Dyn. Earthq. Eng*., **95**, 167-179. https://doi.org/10.1016/j.soildyn.2017.01.009.
Takahashi, A. and Takemura, J. (2005), "Liquefaction-induced large displacement of pile-supported wharf", *Soil Dyn. Earthq. Eng*., **25**(11), 811-825. https://doi.org/10.1016/j.soildyn.2005.04.010.
Tokimatsu, K., Suzuki, H. and Sato, M. (2005), "Effects of inertial and kinematic interaction on seismic behavior of pile with embedded foundation", *Soil Dyn. Earthq. Eng*., **25**(7-10), 753-762. https://doi.org/10.1016/j.soildyn.2004.11.018.
Tran, N.X., Bong, T. and Kim, S.R. (2022), "Kinematic and inertial interaction of single and group piles in slope by displacement phase relation", *J. Earthq. Eng*., **26**(7), 3639-3659. https://doi.org/10.1080/13632469.2020.1813661.
Vytiniotis, A., Panagiotidou, A.I. and Whittle, A.J. (2019), "Analysis of seismic damage mitigation for a pile-supported wharf structure", *Soil Dyn. Earthq. Eng*., **119**, 21-35. https://doi.org /10.1016/j.soildyn.2018.12.020.
Ye, J. and Wang, G. (2015), "Seismic dynamics of offshore breakwater on liquefiable seabed foundation", *Soil Dyn. Earthq. Eng*., **76**, 86-99. https://doi.org/10.1016/j.soildyn.2015.02.003.
Ye, J.H. and Jeng, D.S. (2013), "Three-dimensional dynamic transient response of a poro-elastic unsaturated seabed and a rubble mound breakwater due to seismic loading", *Soil Dyn. Earthq. Eng*., **44**, 14-26. https://doi.org/10.1016/j.soildyn.2012.08.011.
Yoo, M.T., Cha, S.H., Kim, M.M., Choi, J.I. and Han, J.T. (2012). "Evaluation of dynamic group-pile effect in dry sand by centrifuge model tests", *Int. J. Offshore Polar Eng.*, **22**(2).
Yoo, M.T., Choi, J.I., Han, J.T. and Kim, M.M. (2013). "Dynamic py curves for dry sand from centrifuge tests", *J. Earthq. Eng.*, **17**(7), 1082-1102. https://doi.org/10.1080/13632469.2013.801377.
Yoo, M.T., Han, J.T., Choi, J.I. and Kwon, S.Y. (2017), "Development of predicting method for dynamic pile behavior by using centrifuge tests considering the kinematic load effect", *Bull. Earthq. Eng*., **15**(3), 967-989. https://doi.org/10.1007/s10518-016-9998-0.
Yun, J.W. and Han, J.T. (2021), "Evaluation of soil spring methods for response spectrum analysis of pile-supported structures via dynamic centrifuge tests", *Soil Dyn. Earthq. Eng*., **141**, 106537. https://doi.org/10.1016/j.soildyn.2020.106537.
Yun, J.W., Han, J.T. and Kwan, J. (2022a), "Evaluation of the virtual fixed-point method for seismic design of pile-supported structures", *KSCE J. Civil Eng.*, **26**(2), 596-605. https://doi.org/10.1007/s12205-021-0422-1.
Yun, J.W., Han, J.T. and Kim, D.Y (2022b), "Evaluation of seismic p-$y_p$ loops of pile-supported structures installed in saturated sand", *Geomech. Eng.,* **30**(6), 579-586. https://doi.org/10.12989/gae.2022.30.6.579.
Yun, J.W., Han, J.T. and Kim, S.R. (2019), "Evaluation of virtual fixed points in the response spectrum analysis of a pile-supported wharf", *Géotechnique Lett.*, **9**(3), 238-244. https://doi.org/10.1680/jgele.19.00013.

*IC*